Exploring molecular motors and switches at the single-molecule level

ARTICLE *in* MICROSCOPY RESEARCH AND TECHNIQUE · NOVEMBER 2004

Impact Factor: 1.15 · DOI: 10.1002/jemt.20126 · Source: PubMed

8 AUTHORS, INCLUDING:

Marco Capitanio
European Laboratory for Non-Linear Spectr…
51 PUBLICATIONS **517** CITATIONS
SEE PROFILE

Riccardo Cicchi
INO - Istituto Nazionale di Ottica
77 PUBLICATIONS **901** CITATIONS
SEE PROFILE

Giovanni Romano
University of Florence
35 PUBLICATIONS **625** CITATIONS
SEE PROFILE

Francesco S Pavone
European Laboratory for Non-Linear Spectr…
179 PUBLICATIONS **2,943** CITATIONS
SEE PROFILE

Exploring Molecular Motors and Switches at the Single-Molecule Level

M. CAPITANIO,[1,2*] F. VANZI,[1,3] C. BROGGIO,[1] R. CICCHI,[1,4] D. NORMANNO,[1] G. ROMANO,[5] L. SACCONI,[1,6] AND F.S. PAVONE[1,4]

[1]*L.E.N.S., Università degli Studi di Firenze, 50019 Sesto Fiorentino (FI), Italy*
[2]*Dipartimento di Biologia Animale e Genetica "Leo Pardi", Università degli Studi di Firenze, 50125 Firenze, Italy*
[3]*INFM, Sez. Firenze, 50019 Sesto Fiorentino (FI), Italy*
[4]*Dipartimento di Fisica, Università degli Studi di Firenze, 50019 Sesto Fiorentino (FI), Italy*
[5]*Dipartimento di Fisiopatologia Clinica-Sez. di Fisica Medica, Università degli Studi di Firenze, 50100 Firenze, Italy*
[6]*Dipartimento di Fisica, Università di Trento, 38050 Povo (TN), Italy*

KEY WORDS motor proteins; optical tweezers; magnetic and optical wrenches; particle tracking

ABSTRACT Single-molecule techniques have propelled an impressive number of biophysical studies during the last decade. From relatively simple video-microscopy techniques, to sophisticated manipulation and detection apparata, single-molecule techniques are capable of tracking the movements and the reaction trajectories of single enzymatic units. By observing microspheres attached to biomolecules it is possible to follow the motion of molecular motors, or to detect conformational "switching" induced by regulatory proteins. Micromanipulation tools like optical tweezers have been widely applied to understand the mechanisms of linear molecular motors, and have allowed the measurement of the elementary steps and the forces produced by several motor proteins, including myosin, kinesin, and dynein. New experimental assays based on magnetic or optical "wrenches," which are able to apply and detect torques on rotary motors and biopolymers, are opening new possibilities in this field. Here, established and emerging magneto-optical manipulation and video-tracking techniques are reviewed, in the perspective of single molecular motors and regulatory proteins studies. *Microsc. Res. Tech. 65:194–204, 2004.*

INTRODUCTION

A modern picture of a living cell could well resemble life inside a big metropolis, where an incredible variety of subjects with distinct specialized functions work contemporaneously, interacting through a tangled web of interconnections. In living cells, those subjects are constituted by regulatory proteins and enzymes. Many functions fundamental for cell life performed by enzymes (for example DNA transcription, protein synthesis, or cellular trafficking) involve production of work and movement. The capability of converting the chemical energy contained in molecules like ATP or GTP into mechanical work has earned these enzymes the name "molecular motors" (or "motor proteins"). Interactions of motor proteins with other molecules regulate their function: in fact, as in the metropolis example above, a highly complex system requires fine tuning of the localization and activity of all its components. This requires the activity of regulatory proteins. For example, expression of specific genes can be switched off or on by proteins that bind to the DNA molecule and stop or promote DNA transcription. In this sense, such regulatory proteins are "molecular switches."

Classical biochemistry and biophysics take an ensemble picture of cells or of isolated groups of enzymes and extrapolate from a model the behaviour of the single subject. This approach has led and is still leading to great advances in our understanding of many cellular and molecular processes. However, interpreting signals averaged over large (and often heterogeneous) populations of molecules does not always allow a full understanding of the molecular mechanism of action of an enzyme. During the last 10 years, proliferation and establishment of single-molecule techniques have overcome this limit, enabling to directly monitor mechanical and biochemical transitions of single enzymatic units.

Since their development, optical tweezers (Ashkin et al., 1986) have been demonstrated to be a powerful tool for manipulating and investigating single biomolecules. Optical tweezers essentially consist of a laser beam focalised to a sub-micron spot by a high numerical aperture objective; dielectric particles in the range of 10 nm to 10 μm are stably trapped near the beam focus and the displacement and force applied to the particle can be measured with nanometre and piconewton sensitivity, respectively. Forces and displacements exerted by a single biomolecule can be directly measured using functionalised microbeads trapped in the optical tweezers and attached to the molecule. Initial applications of this technique involved the study of

*Correspondence to: M. Capitanio, L.E.N.S., Università degli Studi di Firenze, Via Nello Carrara 1, 50019 Sesto Fiorentino (FI), Italy.
E-mail: capitan@lens.unifi.it

Received 2 October 2004; accepted in revised form 18 October 2004

Contract grant sponsors: INFM, EU; Contract grant numbers: "SINPHYS" PAIS 2002, HPRI-CT-1999-00111 CE.

DOI 10.1002/jemt.20126

Published online in Wiley InterScience (www.interscience.wiley.com).

the motor proteins myosin (Finer et al., 1994) (which drives muscle contraction), kinesin (Svodoba et al., 1993) (involved in intracellular trafficking), dynein (Sakakibara et al., 1999) (responsible for movement of eukaryotic cilia and flagella), and RNA polymerase (Yin et al., 1995) (responsible of transcribing a DNA template into messenger RNA).

Tweezers can apply forces and measure displacements of linear motors; when the system under study performs angular displacements, like in the case of rotary motors, or when twist has to be imposed on the molecule, another class of manipulation tools is needed, which we name "wrenches." A magnetic wrench has been used, for example, to impose different levels of twist to a single DNA molecule and measure the correspondent elastic response (Strick et al., 1996); in that experiment, one end of the DNA molecule was attached to a coverslide surface, while the other end was attached to a magnetic microbead and its rotation controlled by a magnetic field. Wrenches would become a much more powerful tool if they could, analogously to optical tweezers, not only work as manipulators, but also measure angular displacements and torques with mrad and pNnm sensitivity, respectively. Recently developed magnetic (Romano et al., 2003) and optical (LaPorta and Wang, 2004) wrenches seem promising in this respect.

Both tweezers and wrenches imply some sort of manipulation of the molecules under study; when molecules need to be investigated with no net force or torque applied, single-molecule tracking techniques can be used instead. This is particularly useful when studying molecular switches that do not produce net work and cannot thus actively operate against loads. Single-molecule tracking can be achieved by means of fluorescence imaging (not considered in this review; extensive reviews on the field of single-molecule fluorescence can be found elsewhere: Weiss, 1999, 2000), or by probing the molecule position using a microbead attached to the molecule and imaged with conventional video-microscopy. The latter method has been especially applied in a tethered particle motion (TPM) scheme, where a microbead is tethered to a microscope coverslide through a bio-polymer (typically DNA or RNA); conformational changes in the polymer are thus tracked through the microbead motion. The nanometre resolution achievable with this technique allowed, for example, the study of transcription by single molecules of RNA polymerase (Schafer et al., 1991), protein synthesis by single ribosomes (Vanzi et al., 2003), or the interaction of Lac-repressor with a single DNA molecule (Finzi and Gelles, 1995).

In this review, we focus on established and emerging magneto-optical manipulation and video-tracking techniques, viewed in the perspective of single-molecular motors studies and of the regulatory functions of single-molecular switches.

MOLECULAR MOTORS PULLED BY OPTICAL TWEEZERS

Analogously to a massive body in movement, laser beams carry an optical momentum that can be transferred to a particle and that contributes to the forces applied by optical tweezers.

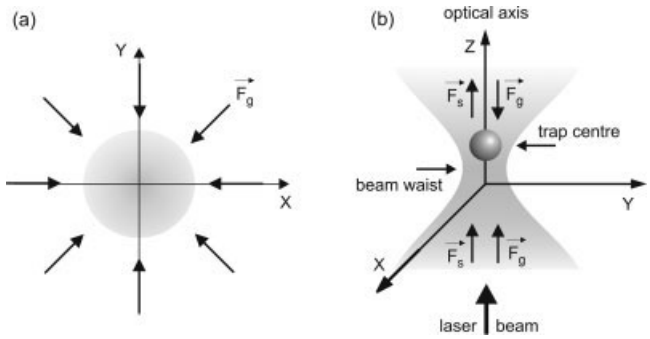

Fig. 1. Configuration of the forces in optical tweezers. **a:** In the *x-y* plane, orthogonal to the direction of propagation of the laser beam, only the gradient force is present, directed towards the beam axis. **b:** Along the optical axis, gradient force is directed towards the beam focus, whereas scattering force is directed towards the direction of propagation of the laser beam. For this reason, the trap centre is positioned slightly above the *x-y* plane.

Forces near the waist of a highly focussed laser beam result from balancing of a scattering force, directed towards the propagation direction of the laser beam, and a gradient force, directed towards the focal point. When the gradient force dominates over the scattering force, dielectric particles can be stably trapped near the beam focus (Fig. 1). The higher the divergence angle from the focal point, the higher the gradient force; for this reason, high-numerical aperture objectives are used to focus the laser light, and optical tweezers are thus naturally integrated within conventional optical microscopes. The resulting trapping force F depends linearly on the displacement x of a trapped microbead, i.e., $F = -k \cdot x$, where k is the trap stiffness. Several techniques have been developed to measure the bead displacement x (Denk and Webb, 1991; Gittes and Schmidt, 1998a; Kamimura, 1987), and to calibrate the trap stiffness k (Capitanio et al., 2002; Ghislain et al., 1994; Gittes and Schmidt, 1998b); once k is known, F is directly measured from the bead displacement x.

In the current view, molecular motors usually work in a biochemical cycle tightly coupled to mechanical transitions of the molecule, where a step (or working stroke) is performed for every ATP or GTP molecule split (Howard, 2001). Optical tweezers can apply forces from few femtonewton to hundreds of piconewtons and measure displacements from about one nanometer to hundreds of nanometers. The range of forces applied by optical tweezers and the range of measurable displacements is ideal for the investigation of mechanical properties of molecular motors. In fact, forces of up to some tens of pN would be predicted from the utilization of the energy available in an ATP molecule with a mechanical step of a size ranging in the nanometers or tens of nanometers (as expected of a molecule of the size of kinesin or myosin, for example). For this reason, optical tweezers have, in fact, proved to be an extremely powerful tool in the study of molecular motors, allowing, for example, to establish that myosin II proceeds along an actin filament with 5–6-nm steps (Molloy et al., 1995), while myosin V performs steps of 36 nm (Mehta et al., 1999). Such working strokes are force-producing transitions that have been quantified

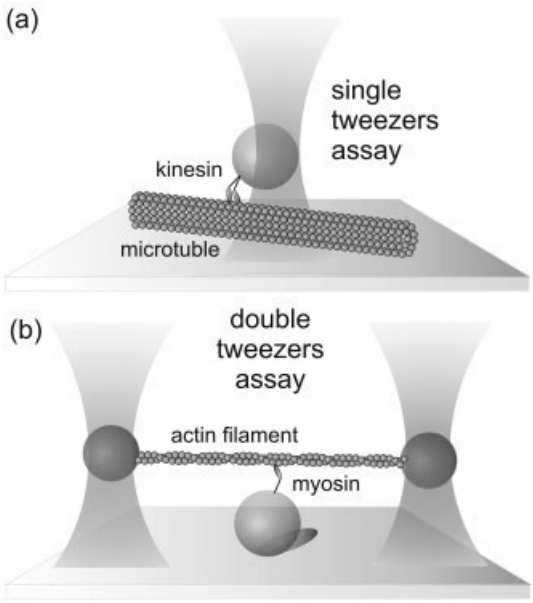

Fig. 2. **a:** The single-tweezers assay used to study processive motors. **b:** The three-beads assay used to study non-processive motors.

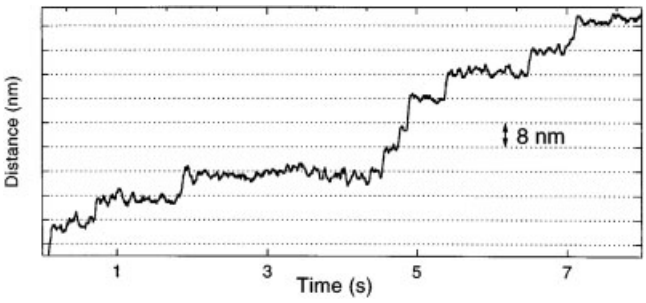

Fig. 3. Position recording of a trapped bead pulled by a single kinesin molecule. Single 8-nm steps are clearly distinguishable, separated by varying dwell time intervals. Reproduced from Schnitzer and Block (1997) Nature 388:386–389, with permission of the publisher (http://www.nature.com).

for a single kinesin, myosin, or RNA polymerase molecule to be, respectively, about 5–6 pN (Svodoba et al., 1993), 3.5 pN (Finer et al., 1994), and 14–25 pN (Wang et al., 1998; Yin et al., 1995).

Molecular motors can be classified in processive and non-processive, depending on the average number of steps P_n taken on their track before diffusing away (Veigel et al., 2002). The processivity number P_n is close to one for non-processive motors (for example, skeletal muscle myosin II), and much greater than one for processive motors (for example, kinesin or myosin V). During the last 10 years, two major optical tweezers assays have been developed to investigate, respectively, processive and non-processive motors (Fig. 2).

A single-tweezers assay has been used to study processive motors like kinesin or myosin V. In this case, the track on which the processive motor walks (a microtuble or an actin filament) is attached to a coverslide surface, while the motor protein is fixed on a trapped bead (Fig. 2a). In the experiment of Svoboda et al. (1993), a microbead carrying a single kinesin molecule was deposited on a microtubule using optical tweezers and the motor movement was detected from the displacement of the bead with respect to the trap centre. Attachment of the molecule to its track resulted in displacement records of kinesin processing along the microtubule that clearly showed a stepwise motion with regular steps of ~8 nm (Fig. 3).

Evolution of the simple single-tweezers assay allowed the processivity of a kinesin molecule to be studied under isotonic conditions. By inserting two crossed acousto-optic modulators (AOMs) in the laser beam path, Lang et al. (2002) controlled the position of the optical trap in the focal plane of the objective with sub-nanometre accuracy. A force clamp feedback monitored the *xy* position of the bead and drove the AOMs in order to impose a constant force on the kinesin molecule. Using this apparatus, Block et al. (2003) subjected a single kinesin molecule to forces in different directions: while lateral and forward forces had only little effect on the molecule processivity, backward forces significantly slowed the molecule, leading to stall at ~8 pN.

The simple single-tweezers assay cannot be used to study non-processive motors: in fact, non-processive motors attach to the filament, perform their working stroke, and then detach from the filament. Even if the bead is spatially constrained near the filament by the optical tweezers, rotational Brownian motion rapidly displaces the molecule away from the filament when it detaches. In 1994, Finer et al. developed a "three-bead assay" to study the interactions of the non-processive myosin II motor with an actin filament (Fig. 2b). In this case, a single actin filament is stretched between two microbeads held by a double optical tweezers (forming a structure named "dumbbell") and presented to a third bead attached to the coverslide, which carries on average one myosin molecule.

Double optical tweezers can be realized by using different approaches: Finer et al. (1994) used a beam-splitter to divide a single laser source in two separate beams; Visscher et al. (1996) realized a double trap by using two separate laser sources. Alternatively, a time-shared configuration may be used, where the laser trap switches rapidly between two or more different positions in the sample plane. This gives a stable double or multiple optical tweezers, if the time taken to scan the different trap positions is much smaller than the diffusion time of the trapped particles. Time-shared traps can be obtained by deflecting the laser beam using galvano mirrors (Sasaki et al., 1991), piezoelectric mirrors (Mio et al., 2000), or AOMs (Capitanio et al., 2004a; Guilford et al., 2004; Nambiar and Meiners, 2002; Visscher et al., 1996).

In a three-bead assay, position recordings of the trapped beads contain single interactions that are correctly detected by reduction in Brownian noise of the bead position (Molloy et al., 1995) (Fig. 4 Left). In fact, compliant traps (~0.05 pN/nm) are used to apply small forces to the molecule and resulting Brownian fluctuations of the dumbbell

$$\left(\sqrt{\langle x^2 \rangle} = \sqrt{\frac{k_B T}{k_r}} \approx 9 \text{ nm} \right)$$

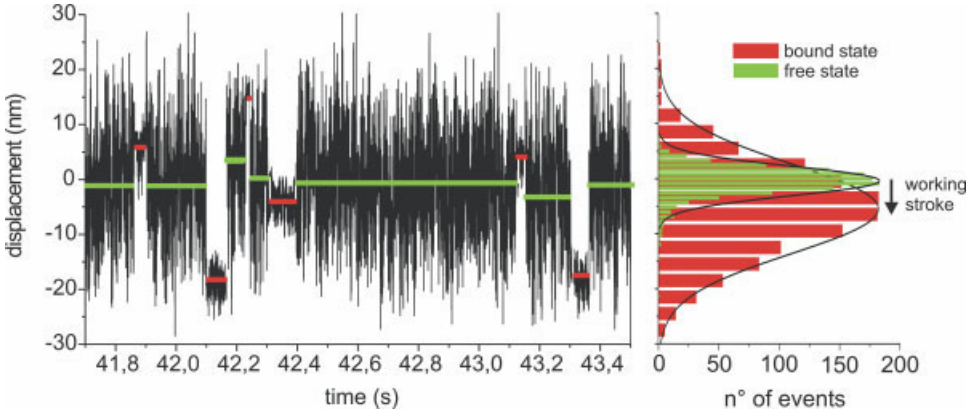

Fig. 4. **Left:** Two seconds of a position recording of one bead of the dumbbell, while a single myosin molecule is interacting with the actin filament in the presence of 5 μM [ATP]. The variance of the position signal has been fitted with a two-state function (free state = high variance, bound state = low variance) using a hidden-Markov algorithm, in order to separate bound from unbound states. Green lines represent the mean position of the free states, whereas red lines represent the mean positions of bound states. **Right:** The distribution of the mean position of bound (red bars) and unbound states (green bars) from a position recording containing 1,213 interactions. The working stroke of the molecule is obtained from the difference between the mean position value of the bound and free states (unpublished data). [Color figure can be viewed in the online issue, which is available at www.interscience.wiley.com.]

are bigger than the myosin working stroke (5–6 nm). For this reason, it is not possible to correctly detect interactions from displacements in position recordings, like originally done by Finer et al. (1994). As evidenced by Molloy et al. (1995), when the myosin molecule binds to the actin filament, a reduction in position noise is clearly visible, due to the higher stiffness of the molecule (~1 pN/nm; Veigel et al., 1998) with respect to the tweezers. Using a threshold on the position variance (Molloy et al., 1995), or fitting the position variance with a two-state function and a hidden-Markov algorithm (D.A. Smith et al., 2001), it is thus possible to separate bound and unbound states. The distance in the mean position distribution of bound and unbound states represents the working stroke of the molecule (Fig. 4 Right).

As demonstrated by Steffen et al. (2001), the situation is even more complicated because of the helical structure of the actin filament: Actin is a polymer formed by G-actin monomers disposed along a helix and spaced ~5.6 nm; the half-pitch of the helix is 36 nm (Moore et al., 1970). Myosin binds stereospecifically to each actin monomer with a rate that depends on the relative orientation of the two molecules. When the relative position of the actin filament and of the myosin molecule is controlled within one nanometre, mean positions of bound events clearly show a distribution with 5.6-nm spaced peaks, modulated at a higher frequency on target zones positioned every 36 nm (Steffen et al., 2001) (Fig. 5). The nanometre stability necessary to evidence this effect can be accomplished using an image-based feedback system (Capitanio et al., 2004b).

Kinesin and skeletal myosin II are probably the most studied motor proteins at the single-molecule level, but many other motors have been investigated during the last years using the optical tweezers assays described previously. In particular, the study of so-called non-conventional myosins Myosin I (Veigel et al., 1999), smooth myosin II (Guilford et al., 1997; Veigel et al., 2003), cardiac myosin (Palmiter et al., 1999), myosin V (Mehta et al., 1999; Rief et al., 2000; Tanaka et al., 2002; Veigel et al., 2002), and myosin VI (Rock et al., 2001) has allowed elucidation of some aspects important for molecular motors functionality, like strain-dependent biochemical steps (Veigel et al., 2003) and working strokes performed in a two-step fashion (Veigel et al., 1999).

TWISTING BIOMOLECULES WITH MAGNETIC AND OPTICAL WRENCHES

Enzymatic activities in cells do not only produce linear motion and force, but also involve rotational motion and torque production. Moreover, torsional strain on biopolymer tracks like DNA is often applied by molecular motors (Harada et al., 2001; Revyakin et al., 2004) or regulatory and structural proteins. On the other hand, torsional strain can modulate the processivity of motors proceeding along the polymer (Li et al., 2003) or the kinetics of molecular switches (Lia et al., 2003). For this reason, an experimental framework capable (analogously to optical tweezers) of contemporaneously applying and measuring torque on microspheres attached to single biomolecules would be highly relevant.

During the few last years, different experimental geometries have been adopted to apply or to measure torque on single biomolecules. One of the most studied rotary motors is the ATP synthase enzyme, which synthesizes ATP from ADP and inorganic phosphate using the proton flow through a membrane as its energy source. The fraction F1-ATPase of ATP synthase can perform the reversal task, at least in vitro, by hydrolysing ATP molecules to pump protons in the opposite direction. F1-ATPase has been shown to be a rotary motor, with a central rotor, formed by its γ-subunit, which rotates in a stator barrel, formed by three α and three β subunits. Noji et al. (1997) directly observed the rotational motion of single F1-ATPase molecules in presence of ATP, by attaching a fluorescent actin filament to the γ-subunit. Itoh et al. (2004) attached a

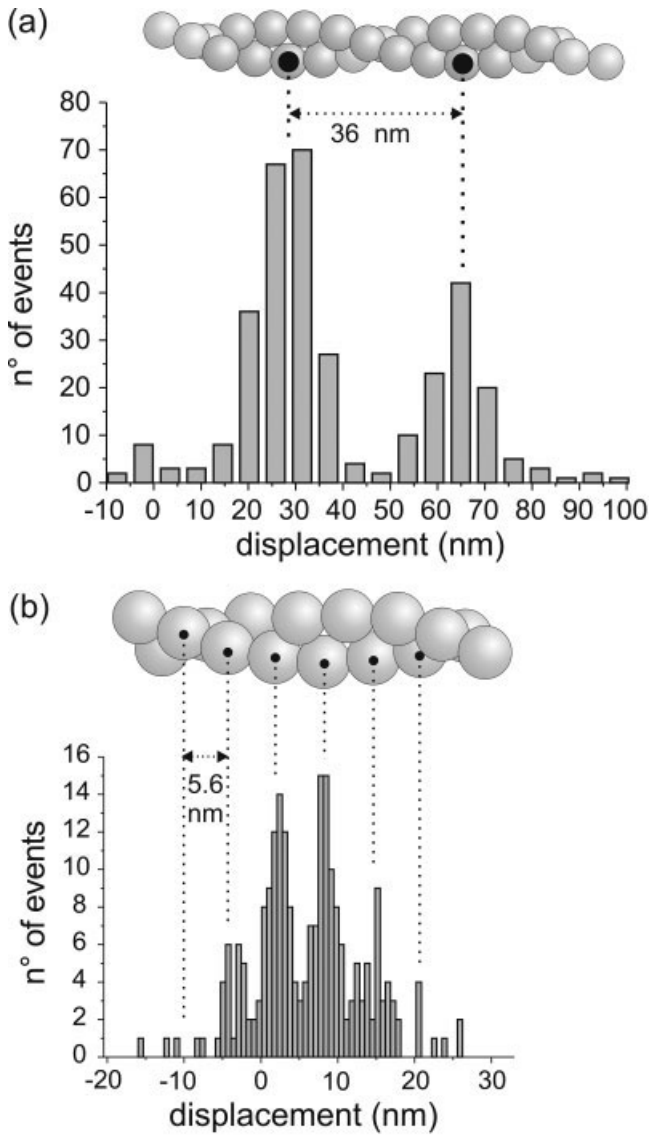

Fig. 5. **a:** The distribution of bound events sampled at 5-nm steps evidences that the myosin molecule preferably binds on target zones spaced about 36 nm (half of the actin periodicity). **b:** The distribution of bound events sampled at 0.5-nm steps shows that the myosin molecule binds to specific sites spaced 5.6 nm, in correspondence with the actin monomers disposed along the filament (unpublished data).

magnetic bead to the γ-subunit of isolated F1-ATPase and rotated the bead using a magnetic wrench. Rotation of the γ-subunit in the proper direction resulted in ATP synthesis, as detected by a luciferase-luciferin reaction (Itoh et al., 2004).

A magnetic wrench was used also by Strick et al. (1998) to study the behaviour of supercoiled and stretched DNA. One end of the DNA molecule was anchored to a glass coverslide and the other end to a magnetic bead; the degree of supercoiling was controlled through the rotation of the magnetic field, while the stretching force was controlled by means of the magnetic field amplitude.

Tsuda et al. (1996) determined the torsional rigidity of actin filaments by measuring the rotational Brownian motion of microbeads tethered to the surface of a microscope coverslip through a single actin filament. Rotation of 2-μm beads sparsely covered with fluorescent 10-nm beads was detected from fluorescence images of the microbeads projected on a silicon intensified target camera. Using the same rotation detection scheme, Harada et al. (2001) observed DNA rotation during transcription by *Escherichia coli* RNA polymerase.

The experimental schemes described above enabled applying torque or, alternatively, measuring angular displacements. A more complex geometry has been used by Bryant et al. (2003) in order to both apply twist and measure torsional rigidity of a single DNA molecule (Fig. 6a). A DNA construct with three different attachment sites and a nick was stretched between two microbeads held by a rotating micropipette and optical tweezers. A sub-micron bead, which acted as a rotor, was attached just above the nick, which acted as a swivel. The micropipette was rotated by more than 300 turns while the rotor bead was held by hydrodynamic flow, in order to build up torsional stress in the upper part of the molecule. When the flow was released, the rotor bead started rotating and from its angular velocity the torque was measured as a function of the imposed twist (Fig. 6b). The torque depends linearly on the twist angle in the range between −9.6 and 34 pNnm, where the DNA molecule is in the B conformation. From the slope of the torque-twist curve, a twist elasticity of 410 $pNnm^2rad^{-1}$ is derived. For torques higher than 34 pNnm or smaller than −9.6 pNnm, the DNA molecule undergoes a constant-torque structural transition towards the P conformation (Fig. 6c).

Besides the biological results reported above, during the last years novel magnetic and optical wrenches have been developed that seem promising with respect to combining in a simple and general framework torsional manipulation with rotation and torque detection.

Magnetic wrenches use the well-known phenomenon of magnet orientation along a magnetic field, like in the case of a compass needle oriented by the earth magnetic field. In this respect, ferromagnetic and superparamagnetic beads act as micromagnets in a homogeneous magnetic field (Normanno et al., 2004). In magnetic wrenches where the magnetic field is not homogeneous, a force directed towards the field gradient is also exerted on the magnetic bead. This force cannot produce a three-dimensional potential well, but has anyway been used to manipulate biomolecules (Gosse and Croquette, 2002).

Sacconi et al. (2001) built a magneto-optic manipulator that combines optical tweezers with a magnetic wrench. Superparamagnetic beads can be trapped in three dimensions by the optical tweezers and contemporaneously rotated around the three axes by the magnetic wrench. Forces up to 230 pN and force momenta up to 10^{-16} N · m can be applied. The optical tweezers and the magnetic wrench are decoupled, since the magnetic field is almost homogeneous inside the trapping region. An interferometric rotation detection scheme and a torque calibration procedure enable the direct measurement of angular deviations and applied external torque on the trapped bead with high sensitivity

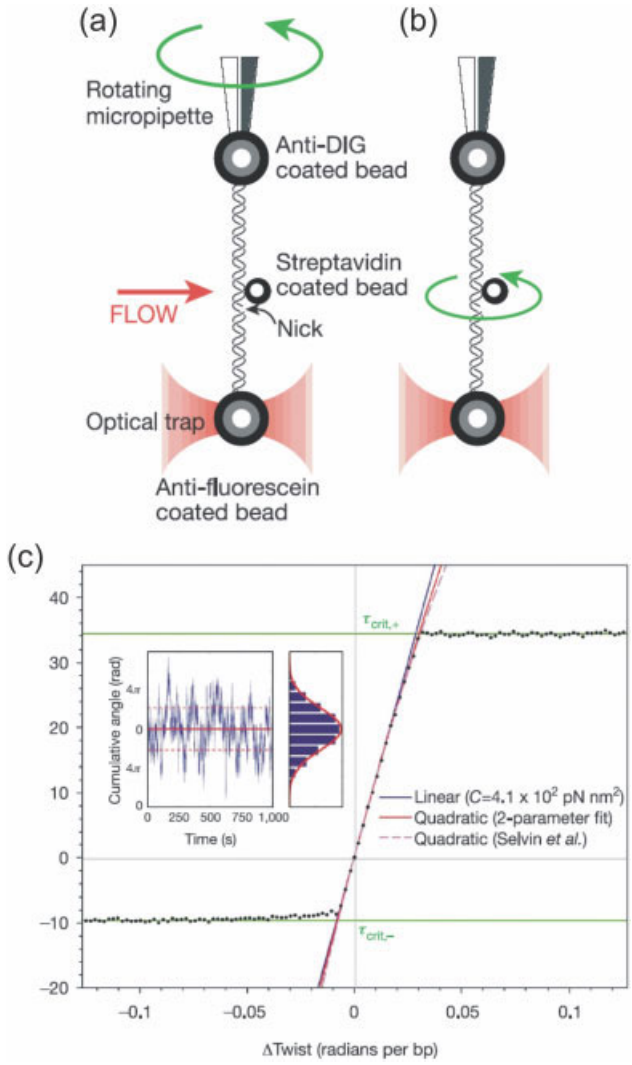

Fig. 6. **a:** Each molecule was stretched between two antibody-coated beads using a dual-beam optical trap. A rotor bead was then attached to the central biotinylated patch. The rotor was held fixed by applying a fluid flow, and the micropipette was twisted to build up torsional strain in the upper segment of the molecule. **b:** Upon releasing the flow, the central bead rotated to relieve the torsional strain. **c:** Averaged twist elasticity data. Green lines, constant-torque structural transitions. Blue, linear fit to the data points falling within ±8 pN nm. Anharmonic models give superior fits to the data over the full range of B-DNA stability. Red, two-parameter anharmonic fit; dashed purple, one-parameter anharmonic fit (Bryant et al., 2003). Reproduced from Bryant et al. (2003) Nature 424:338–341, with permission of the publisher (http://www.nature.com). [Color figure can be viewed in the online issue, which is available at www.interscience.wiley.com.]

and fast time response. The magnetic wrench applies a torque

$$\Gamma^{mag} = -k_{rot}\theta,$$

where k_{rot} is the rotational stiffness of the magnetic manipulator and θ is the angle between the applied magnetic field and a reference axis fixed on the bead. The angle θ can be measured from the phase shift between the magnetic field rotation signal and the bead rotation signal, while k_{rot} can be calibrated against rotational viscous drag. Γ^{mag} can thus be directly obtained from the angle θ (Fig. 7). Until now, the apparatus has been used to directly measure the torque induced by elliptically polarized light to trapped superparamagnetic microbeads (Capitanio et al., 2004c; Normanno et al., 2004).

Optical wrenches rely on the angular momentum carried by laser beams. Optical angular momentum exists in two forms: orbital angular momentum, carried by laser beams with a helical phase structure, or spin angular momentum, carried by elliptically polarized beams. Torque is transferred to the trapped particle through absorption of orbital (He et al., 1995) or spin angular momentum (Friese et al., 1998a), or by scattering of angular momentum in different states (Friese et al., 1998b; Santamato et al., 2002). Depending on the physical effect the optical wrench relies on, either angular trapping or continuous rotation can be applied to the microbead.

La Porta and Wang (2004) developed an optical device that is capable of operating both as optical tweezers and as optical wrench on quartz microparticles. Angular trapping is based on the interaction between linearly polarized light and a birefringent quartz particle. Misalignment between the electric field of the laser beam and the polarization induced on the particle results in a torque that tends to tilt the particle extraordinary axis towards the electric field, an effect already observed by Friese et al. (1998b). The orientation of the laser polarization can be varied very rapidly using a polarization rotator based on AOMs. Angular trapping is combined with a high-bandwidth rotation detector, similar to that reported by Bishop et al. (2003), which can be calibrated to directly measure angular displacements and torque. Moreover, a digital feedback loop that uses the signal from the torque detector to drive the polarization rotator can be exploited to clamp the applied torque at defined stable levels.

MOLECULAR MOTORS AND SWITCHES TRACKED BY VIDEO-MICROSCOPY

In the tethered particle motion (TPM) method, a microsphere is tethered to the surface of a microscope coverslip through a single biopolymer (for example DNA or RNA). As a consequence of tethering, the Brownian diffusion of such microsphere is restricted within a volume that is proportional to the length of the polymer itself. An accurate measurement of the volume explored by the microsphere in its diffusion, therefore, can report on the length of the polymer and its variations due to interactions with proteins or to changes in the physical and chemical properties of the surrounding buffer. This method was first developed by Schafer et al. (1991) to study the activity of RNA polymerase at the single-molecule level. In addition to further studies on RNA polymerase (Tolic-Norrelykke et al., 2004; Yin et al., 1999), the method has been applied also to the single-molecule study of Lac repressor (Finzi and Gelles, 1995), RecBCD (Dohoney and Gelles, 2001), ribosomes (Vanzi et al., 2003), and RuvA (Pouget et al., 2004).

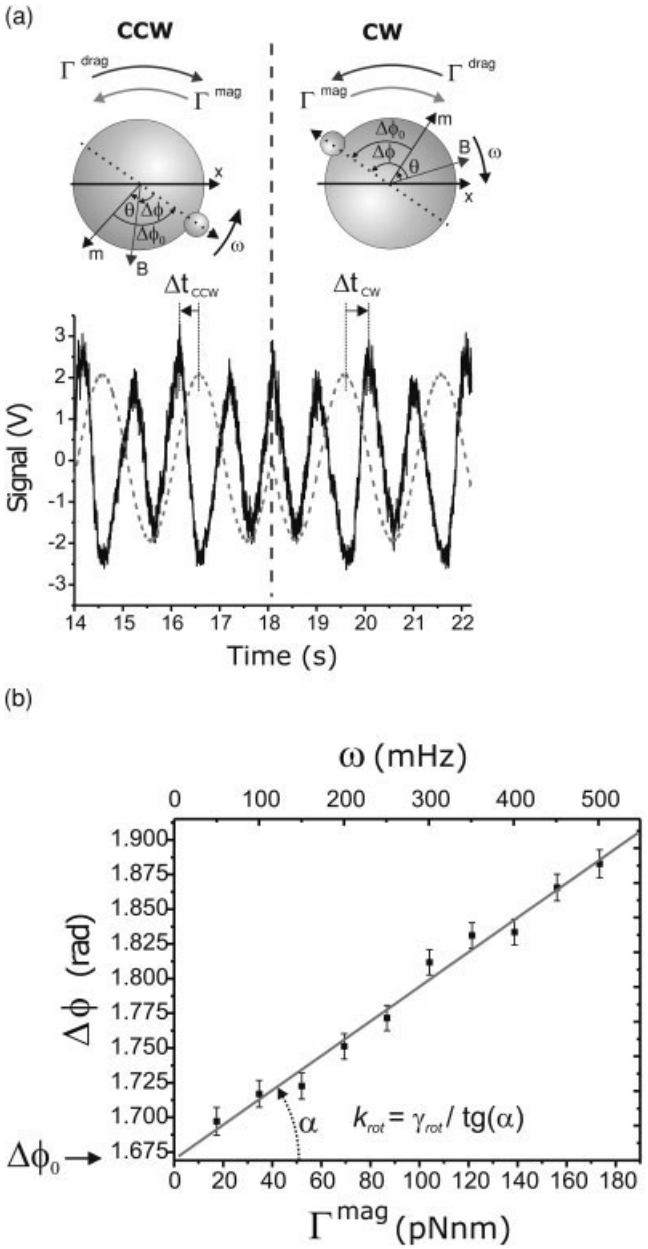

Fig. 7. Calibration of the magnetic wrench. **a:** Detection of bead rotation is achieved on slightly asymmetric beads by means of a differential interference contrast (DIC) technique. Calibration is performed against rotational viscous drag, by rotating the magnetic bead either clockwise (CW) or counter-clockwise (CCW) at different angular velocities. The angle θ is measured as $\theta = |\Delta\phi| - \Delta\phi_0$. $\Delta\phi$ is defined as $\Delta\phi = \omega \cdot \Delta t$, where Δt is the time difference between the non-linear fit maximum of the bead rotation signal (continuous line) and the maximum of the current monitor signal (dotted line) driving the rotation of the magnetic field B. The small impurity in the upper part of the figure represents the bead asymmetry. The rotation of the bead impurity and of the B field corresponds in the lower part, respectively, to the continuous and dotted line. When $\Gamma^{drag} = 0$, m and B are aligned and $|\Delta\phi| = \Delta\phi_0$. **b:** From the slope of the curve $\Delta\phi$ the rotational stiffness is obtained, whereas from the intercept, $\Delta\phi_0$ is obtained.

The appeal of this method mainly derives from the relative simplicity of implementation with respect to other single-molecule techniques, while maintaining some of the advantages of those techniques. In fact, TPM allows measurements of the reaction trajectories of single enzymes using the observation of the diffusion of a microsphere in a simple transmission or differential interference contrast (DIC) microscope. Additionally, the TPM method offers the opportunity of collecting single-molecule data from a large number of molecules simultaneously (by measuring the Brownian diffusion of many tethered microspheres present in one microscope field). This drastically increases the efficiency of single-molecule data collection with respect to the other methods in which only one molecule at a time can be investigated.

In its first implementation on RNA polymerase (Schafer et al., 1991), the method was based on imaging sub-micron-size gold or polystirene beads (50–250 nm diameter) with a DIC microscope and acquiring videos of their brownian motion. The range of diffusion was then quantified by digital image processing. Video frames over a chosen interval of time (for example 4.3 s in the RNA polymerase experiments described by Schafer et al., 1991) were averaged and the resulting image was fitted with a 2D Gaussian function, whose standard deviation along the two axis (compared to a similar analysis performed on an immobilized bead) provided quantitative information on the volume explored by the microsphere during the time probed. The choice of time interval used for image averaging determines the signal-to-noise ratio achieved and the time resolution limits of the experiments, as discussed below.

Alternatively to determining the range of diffusion of the bead using an average image, analysis of motion can be performed based on determining the centroid position of the bead in each video frame and then quantifying the distribution of positions within a certain time interval (Pouget et al., 2004; Vanzi et al., 2003). With a magnification appropriate to the size of microspheres chosen for the experiments, cross-correlation or thresholded-centroid algorithms allow fast and precise determination of the position of the microsphere. The limit in the precision of this measurement is usually set by mechanical vibrations of the apparatus or small fluctuations and heterogeneities in the illumination of the sample. Standard precautions to reduce these problems allow measurement of the centroid of a 200-nm-diameter polystirene microsphere at a video rate with a precision of 10 nm or less. The parameter most relevant in TPM measurements is the standard deviation of the width of the distribution of positions sampled by the microsphere in its Brownian diffusion. Therefore, analogously to the image processing described above, this method also requires averaging over a time interval sufficiently long for the microsphere to explore the entire volume allowed by the tether. As discussed above, this characteristic time depends on the size of the microsphere and the length of the polymer itself and sets a limit to the time resolution of the technique.

The TPM method has been extensively characterized and calibrated by Yin et al. (1994) using the image averaging method and by Pouget et al. (2004) using the

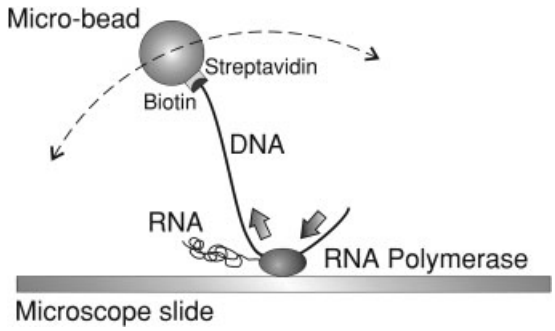

Fig. 8. Schematic representation of a TPM experiment on a processive enzyme. RNA polymerase is attached to the surface of a microscope coverslip and the 5′ end of the DNA template is tagged with a microsphere. The dashed arrows indicate the range of diffusion allowed by the tether. Sliding of the template in the direction shown by the small arrows induces lenghtening of the tether, measurable in TPM by an increase of the range of diffusion of the bead.

centroid tracking method. Here we summarize some fundamental information defining the precision and time resolution of the method. Yin et al. (1994) used microspheres with 0.23-μm diameter, and found that the precision of the TPM measurements (expressed as the square root of the tether length variance in the measurement) scales linearly with a slope of 191-bp $Hz^{-1/2}$ for a DNA molecule of 1,093 base pairs. On the other hand, they also found that averaging over an interval of 4.3 s allows determination of the tether length to within 10% precision in a range of lengths between 400 and 2,000 base pairs. The method is, therefore, viable for measuring enzyme dynamics occurring in the timescale of tens of seconds and inducing, in that timescale, changes of several tens of base pairs in the tether length.

Fast enzymes, such as DNA or RNA polymerase (operating in vitro at rates of 10–20 nucleotides/s) can be studied in a configuration such as that shown in Figure 8, where the polymerase is attached to the surface of a coverslip and the template DNA molecule is labelled at one end with a microsphere. Enzymatic activity causes a time-dependent increase or a decrease of the tether length, for 5′ and 3′ labelled DNA, respectively.

Tolic-Norrelykke et al. (2004) measured the rate of transcription of individual RNA polymerase molecules with a precision of about 1 base pair/s and observed variations in the catalytic rate for the same enzyme over time (for example long pauses) or among different molecules. These measurements illustrate the power of TPM as a single-molecule technique, despite its somewhat limited resolution. Measurement of more subtle kinetic properties of the polymerase (for example backtracking) require the use of higher resolution techniques, i.e., optical tweezers (Shaevitz et al., 2003).

In addition to the study of processive enzymes (such as DNA or RNA polymerase), which induce a monotonic change in the length of the tether, TPM can also be employed for measuring the kinetics of "switches," protein that performs a regulatory function by binding to DNA and changing its structure (for example forming a loop between two specific recognition sequences, as in the case of Lac or Gal repressor). This application of TPM was first introduced by Finzi and Gelles (1995) using a system such as that shown in Figure 9. In these measurements, the presence or absence of a loop between the two operator sequences is revealed by the range of diffusion of the microsphere switching between two discrete levels (Fig. 10). The lifetimes of the looped and unlooped state can be measured, providing information complementary to kinetic and equilibrium measurements performed in solution, where the looped state cannot be distinguished from one in which the repressor is bound to only one operator. The configuration shown in Figure 9 allows measurement of the activity of structural or regulatory proteins capable of binding simultaneously to more than one site on the DNA molecule and inducing, therefore, large changes in the average end-to-end length of the molecule, which can be promptly detected with TPM. With appropriately designed constructs, TPM could also be employed to measure more subtle effects, such as bending of the DNA, induced by regulatory or structural proteins binding to one site, or changes in the persistence length of the DNA due to binding of accessory proteins.

Finally, high-precision 3D tracking of tethered microspheres is also employed, in combination with manipulation tools (optical or magnetic tweezers) for the measurement of stretching forces acting on the tether molecule and, therefore, for investigating the physical properties of nucleic acids (Strick et al., 1998).

CONCLUSIONS AND FUTURE PROSPECTS

The development of a large array of single-molecule manipulation and imaging techniques has had an impressive impact on biochemistry and biophysics in the last few years. Driven mostly by technological advances (for example, in laser and detection technologies), this field has been producing a number of sensational measurements and is now mature to be considered another well-established tool in the hands of biophysicists, physicists, and biochemists.

In the post-genomic era, the capability of adding to the conventional tools of biochemical investigation an array of complementary methodologies for the study and manipulation of proteins at the single-molecule level represents an incredible opportunity to deepen our understanding of biological molecular machines and, perhaps, even to develop new ones.

Single-molecule techniques themselves are highly complementary with each other. The tethered particle method and tracking techniques allow screening of large populations of molecules, while still preserving many of the advantages of the single-molecule techniques. This can be very useful in developing new types of assays for applying, for example, tweezers or other high-resolution techniques to the study of new enzymes. These methods are also well suited to the study of enzymes that behave like switches or induce structural alterations in a target biopolymer to which they bind. Optical tweezers can be used for measurements and manipulation of linear motors, while optical and magnetic wrenches can be employed for similar studies on rotary motors. These instruments allow fine studies

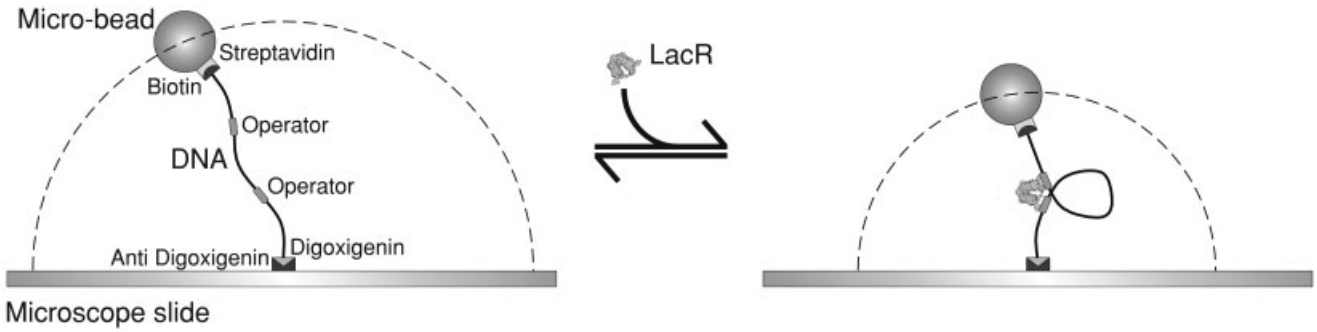

Fig. 9. Schematic representation of TPM experiment on a "switch protein." **Left:** The DNA template is attached at one end to the glass coverslip and is tagged at the other end with a microsphere. The DNA molecule contains two binding sites (shown as empty boxes) for the protein (for example Lac repressor). **Right:** Upon binding of Lac repressor to the two sites simultaneously, a loop is formed in the DNA molecule, the tether is effectively shortened, and the range of diffusion of the bead (shown by the dashed line) is decreased.

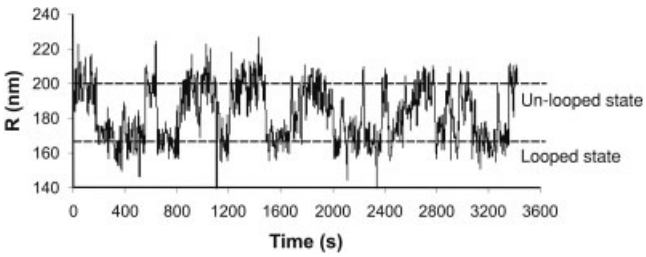

Fig. 10. Example of experimental TPM recording. The radius of mobility of the microsphere is shown as a function of time. The radius was measured using the centroid method described in the text, using a window of 2 s for averaging of the centroid position distribution. The two levels of mobility represent the unlooped and looped state that alternate upon dissociation and association, respectively, of Lac repressor to the DNA molecule as shown in Figure 9 (unpublished data).

on the mechanical activity of motor proteins. Single-molecule fluorescence, on the other hand, has not been treated in this review but is an incredible tool for the investigation of the structural dynamics at the base of the mechanical activity of these proteins. So, the combination of these techniques clearly represents an impressive opportunity for studying the structure-function relationship in many enzymatic systems. Furthermore, these technologies are still evolving at an impressive pace. During the last 10 years, for example, optical tweezers changed from particle micro-manipulators into advanced tools capable of resolving nanometre displacements with sub-millisecond temporal resolution. In recent years, such high detection accuracy has been combined with a comparable stability, which, for example, allowed the single binding sites on actin filaments to be neatly mapped. Optical tweezers have become a well-established technique; nevertheless, forthcoming technological advances can reveal aspects of molecular motors and proteins function yet hidden. For example, attachment of myosin to an actin filament and production of the working stroke is too fast to be resolved by the actual generation of optical tweezers. For this reason, single myosin molecules have not been studied in real isometric conditions. Detection and feedback systems fast enough to reveal and control the position of the lever-arm during the development of the working stroke could also elucidate some still undisclosed aspects of the mechanism of force production in motor proteins. On the other hand, development of a common framework to apply and detect torques on rotary motors and biopolymers would be likely to lead to a wide range of new investigations. Among the interesting open questions still to be answered are, for example, the processivity mechanism of the bacteriophage ϕ29. Bacteriophage ϕ29 packages double-stranded DNA into its capsid by means of a molecular motor that hydrolyses ATP. The motor subunit has been shown to apply high forces, up to 57 pN (D.E. Smith et al., 2001), and has been proposed to be a rotary motor, which couples rotation to DNA translocation (Simpson et al., 2000). Also, conventional myosin II could benefit from single-molecule studies on torque and rotation. In fact, by measuring the collective behaviour of many molecules in isolated muscle fibres, myosin II has been shown to twist along its lever arm during production of the working stroke (Corrie et al., 1999). Such twist of the lever-arm cannot be detected in a classical three-bead assay, but needs a new rotational assay.

Progress in single-molecule investigations will depend not only on technological advances, but also on improvements in biotechnologies and genetics. For example, single-molecule mutational studies, or comparison of natural isoforms with minimal sequence differences, can elucidate precisely the existing relationship between the protein structure and its function. Expression of proteins known only from sequence analysis can also bring new information on molecular motors and regulatory proteins function. Moreover, enzyme functionality depends sensibly on the surface onto which they are deposited. Micro-manipulation techniques always involve attachment of enzymes on a coverslide surface, on a micro-bead or on some sort of "handle." Surface treatment is, therefore, another important aspect to be solved, for example, for the study of complex molecular machines like the ribosome or the preoteosome.

ACKNOWLEDGMENTS

The authors are grateful to Massimo Galimberti for critical reading and useful discussion and acknowledge M. Canepari, P. Cacciafesta, and R. Bottinelli for the biochemical preparations used in the acto-myosin experiments. This work under contract HPRI-CT-1999-00111 CE was partially supported by "SINPHYS" PAIS 2002, project of INFM.

REFERENCES

Ashkin A, Dziedzik JM, Bjorkholm JE, Chu S. 1986. Observation of a single-beam gradient force optical trap for dielectric particles. Opt Lett 11:288–290.

Bishop AI, Nieminen TA, Heckenberg NR, Rubinsztein-Dunlop H. 2003. Optical application and measurements of torque on microparticles of isotropic nonabsorbing material. Phys Rev A 68:33802–33807.

Block SM, Asbury CL, Shaevitz JW, Lang MJ. 2003. Probing the kinesin reaction cycle with a 2D optical force clamp. Proc Natl Acad Sci USA 100:2351–2356.

Bryant Z, Stone MD, Gore J, Smith SB, Cozzarelli NR, Bustamante C. 2003. Structural transitions and elasticity from torque measurements on DNA. Nature 424:338–341.

Capitanio M, Romano G, Ballerini R, Giuntini M, Pavone FS. 2002. Calibration of optical tweezers with differential interference contrast signals. Rev Sci Instrum 73:1687–1696.

Capitanio M, Cicchi R, Pavone FS. 2004a. Continuous and time-shared multiple optical tweezers for the study of single motor proteins. Opt Laser Eng (in press).

Capitanio M, Cicchi R, Pavone FS. 2004b. Position control and optical manipulation for nanotechnology applications. Eur Phys J B (in press).

Capitanio M, Normanno D, Pavone FS. 2004c. High precision measurements of light-induced torque on absorbing micro-spheres. Opt Lett 29:2231–2233.

Corrie JET, Brandmeier BD, Ferguson RE, Trentham DR, Kendrick-Jones J, Hopkins SC, van der heide UA, Goldman YE, Sabido-David C, Dale RE, Criddle S, Irving M. 1999. Dynamic measurement of myosin light-chain-domain tilt and twist in muscle contraction. Nature 400:425–430.

Denk W, Webb WW. 1991. Optical measurements of picometer displacements of transparent microscopic objects. Appl Opt 29:2382–2390.

Dohoney KM, Gelles J. 2001. Chi-sequence recognition and DNA translocation by single RecBCD helicase/nuclease molecules. Nature 409:370–374.

Finer JT, Simmons RM, Spudich JA. 1994. Single myosin molecule mechanics: piconewton forces and nanometer steps. Nature 368: 113–119.

Finzi L, Gelles J. 1995. Measurement of lactose repressor-mediated loop formation and breakdown in single DNA molecules. Science 78:378–380.

Friese ME, Nieminen TA, Heckenberg NR, Rubinsztein-Dunlop H. 1998a. Optical torque controlled by elliptical polarization. Opt Lett 23:1–3.

Friese ME, Nieminen TA, Heckenberg NR, Rubinsztein-Dunlop H. 1998b. Optical alignment and spinning of laser-trapped microscopic particles. Nature 394:348–350.

Ghislain L, Switz NA, Webb WW. 1994. Measurement of small forces using an optical trap. Rev Sci Instrum 65:2762–2768.

Gittes F, Schmidt CF. 1998a. Interference model for back-focal-plane displacement detection in optical tweezers. Opt Lett 23:7–9.

Gittes F, Schmidt CF. 1998b. Signals and noise in micromechanical measurements. Methods Cell Biol 55:129–156.

Gosse C, Croquette V. 2002. Magnetic tweezers: Micromanipulation and force measurement at the molecular level. Biophys J 82:3314–3329.

Guilford WH, Dupuis DE, Kennedy G, Wu J, Patlak JB, Warshaw DM. 1997. Smooth and skeletal muscle myosin produce similar unitary forces and displacements in the laser trap. Biophys J 72: 1006–1021.

Guilford WH, Tournas JA, Dascalu D, Watson DS. 2004. Creating multiple time-shared laser traps with simultaneous displacement detection using digital signal processing hardware. Anal Biochem 326:153–166.

Harada Y, Ohara O, Takatsuki A, Itoh H, Shimamoto N, Kinosita Jr K. 2001. Direct observation of DNA rotation during transcription by *Escherichia coli* RNA polymerase. Nature 409:113–115.

He H, Friese ME, Heckenberg NR, Rubinsztein-Dunlop H, 1995. Direct observation of transfer of angular momentum to absorptive particles from a laser beam with a phase singularity. Phys Rev Lett 75:826–829.

Howard J. 2001. Mechanics of motor proteins and the cytoskeleton. Sunderland, MA; Sinauer Associates, Inc.

Itoh H, Takahashi A, Adachi K, Noji H, Yasuda R, Yoshida M, Kinosita K Jr. 2004. Mechanically driven ATP synthesis by F1-ATPase. Nature 427:465–468.

Kamimura S. 1987. Direct measurements of nanometric displacements under an optical microscope. Appl Opt 26:3425–3427.

Lang MJ, Asbury CL, Shaevitz JW, Block SM. 2002. An automated two-dimensional optical force clamp for single molecule studies. Biophys J 83:491–501.

LaPorta A, Wang MD. 2004. Optical torque wrench: angular trapping, rotation, and torque detection of quartz microparticles. Phys Rev Lett 92:190801–190804.

Li D, Zhao R, Liyestrom W, Gai D, Zhang R, DeCaprio JA, Fanning E, Jochiamiak A, Szakonyi G, Chen XS. 2003. Structure of the replicative helicase of the oncoprotein SV40 large tumor antigen. Nature 423:512–518.

Lia G, Bensimon D, Croquette V, Allemand JF, Dunlap D, Lewis DEA, Adhya S, Finzi L. 2003. Supercoiling and denaturation in Gal repressor/heat unstable nucleoid protein (HU)-mediated DNA looping. PNAS 100:11373–11377.

Mehta AD, Rock RS, Rief M, Spudich JA, Mooseker MS, Cheney RE. 1999. Myosin V is a processive actin-based motor. Nature 400:590–593.

Mio C, Gong T, Terray A, Marr WM. 2000. Design of a scanning laser optical trap for multiparticle manipulation. Rev Sci Instr 71:2196–2200.

Molloy JE, Burns JE, Kendrick-Jones J, Tregear RT, White DCS. 1995. Movement and force produced by a single myosin head. Nature 378:209–212.

Moore PB, Huxley HE, DeRosier DJ. 1970. Three-dimensional reconstruction of F-actin, thin filaments and decorated thin filaments. J Mol Biol 50:279–295.

Nambiar R, Meiners JC. 2002. Fast position measurements with scanning line optical tweezers. Opt Lett 27:836–838.

Noji H, Yasuda R, Yoshida M, Kinosita K Jr. 1997. Direct observations of the rotation of F1-ATPase. Nature 386:299–302.

Normanno D, Capitanio M, Pavone FS, 2004. Spin absorption, windmill and magneto-optics effects in optical angular momentum transfer. Phys Rev A 70:53829.

Palmiter KA, Tyska MJ, Dupuis DE, Alpert NR, Warshaw DM. 1999. Kinetic differences at the single molecule level accounts for the functional diversity of rabbit cardiac myosin isoforms. J Physiol 519:669–678.

Pouget N, Dennis C, Turlan C, Grigoriev M, Chandler M, Salome L. 2004. Single-particle tracking for DNA tether length monitoring. Nucleic Acids Res 32:e73.

Revyakin A, Ebright RH, Strick TR. 2004. Promoter unwinding and promoter clearance by RNA polymerase: Detection by single-molecule DNA nanomanipulation. PNAS 101:4776–4780.

Rief M, Rock RS, Mehta AD, Mooseker MS, Cheney RE, Spudich JA. 2000. Myosin-V stepping kinetics : A molecular model for processivity. Proc Natl Acad Sci USA 97:9482–9486.

Rock RS, Rice SE, Wells AL, Purcell TJ, Spudich JA, Sweeney HL. 2001. Myosin VI is a processive motor with a large step size. Proc Natl Acad Sci USA 98:13655–13659.

Romano G, Sacconi L, Capitanio M, Pavone FS. 2003. Force and torque measurement using magnetic micro beads for single molecule biophysics. Opt Comm 215:323–331.

Sacconi L, Romano G, Ballerini L, Capitanio M, De Pas M, Giuntini M, Dunlap D, Finzi L, and Pavone FS. 2001. Three-dimensional magneto-optic trap for micro-object manipulation. Opt Lett 26: 1359–1361.

Sakakibara H, Kojima H, Sakai Y, Katayama E, Oiwa K. 1999. Inner-arm dynein c of Chlamydomonas flagella is a single-headed processive motor. Nature 400:586–590.

Santamato E, Sasso A, Piccirillo B, Vella A. 2002. Optical angular momentum transfer to transparent isotropic particles using laser beam carrying zero average angular momentum. Opt Express 10: 871–878.

Sasaki K, Masanori M, Misawa H, Kitamura N, Masuhara H. 1991. Pattern formation and flow control of fine particles by laser-scanning micromanipulation. Opt Lett 16:1463–1465.

Schafer DA, Gelles J, Sheetz MP, Landick R. 1991. Transcription by single molecules of RNA polymerase observed by light microscopy. Nature 352:444–448.

Schnitzer MJ, Block SM. 1997. Kinesin hydrolyses one ATP per 8-nm step. Nature 388:386–390.
Shaevitz JW, Abbondanzieri EA, Landick R, Block SM. 2003. Backtracking by single RNA polymerase molecules observed at near-base-pair resolution. Nature 426:684–687.
Simpson AA, Tao Y, Leiman PG, Badasso MO, He Y, Jardine PJ, Olson NH, Morais MC, Grimes S, Anderson DL, Baker TS, Rossmann MG. 2000. Structure of the bacteriophage ϕ29 DNA packaging motor. Nature 408:745–750.
Smith DA, Steffen W, Simmons RM, Sleep J. 2001. Hidden-Markov methods for the analysis of single-molecule acotmyosin displacement data: the Variance-Hidden-Markov method. Biophys J 81: 2798–2816.
Smith DE, Tans SJ, Smith SB, Grimes S, Anderson DL, Bustamante C. 2001. The bacteriophage ϕ29 portal motor can package DNA against a large internal force. Nature 413:748–752.
Steffen W, Smith D, Simmons R, Sleep J. 2001. Mapping the actin filament with myosin. Proc Natl Acad Sci USA 98:14949–54.
Strick TR, Allemand JF, Bensimon D, Bensimon A, Croquette V. 1996. The elasticity of a single supercoiled DNA molecule. Science 271:1835–1837.
Strick TR, Allemand JF, Bensimon D, Croquette V. 1998. Behaviour of supercoiled DNA. Biophys J 74:2016–2028.
Svoboda K, Schmidt CF, Schnapp BJ, Block SM. 1993. Direct observation of kinesin stepping by optical trapping interferometry. Nature 365:721–727.
Tanaka H, Homma K, Iwane AH, Katayama E, Ikebe R, Saito J, Yanagida T, Ikebe M. 2002. The motor domain determines the large step of myosin-V. Nature 415:192–195.
Tolic-Norrelykke SF, Engh AM, Landick R, Gelles J. 2004. Diversity in the rates of transcript elongation by single RNA polymerase molecules. J Biol Chem 279:3292–3299.
Tsuda Y, Yasutake H, Ishijima A, Yanagida T. 1996. Torsional rigidity of single actin filaments and actin-actin bond breaking force under torsion measured directly by in vitro micromanipulation. Proc Natl Acad Sci USA 93:12937–12942.
Vanzi F, Vladimirov S, Knudsen CR, Goldman YE, Cooperman BS. 2003. Protein synthesis by single ribosomes. RNA 9:1174–1179.
Veigel C, Bartoo ML, White DCS, Sparrow JC, Molloy JE. 1998. The stiffness of rabbit skeletal actomyosin cross-bridges determined with an optical tweezers transducer. Biophys J 75:1424–1438.
Veigel C, Coluccio LM, Jontes JD, Sparrow JC, Milligan RA, Molloy JE. 1999. The motor protein myosin-I produces its working stroke in two steps. Nature 398:530–533.
Veigel C, Wang F, Bartoo ML, Sellers JR, Molloy JE. 2002. The gated gait of the processive molecular motor, myosin V. Nature Cell Biol 4:59–65.
Veigel C, Molloy JE, Schmitz S, Kendrick-Jones J. 2003. Load-dependent kinetics of force production by smooth muscle myosin measured with optical tweezers. Nature Cell Biol 5:980–986.
Visscher K, Gross SP, Block SM. 1996. Construction of multiple-beam optical traps with nanometer-resolution position sensing. IEEE J Sel Top Quant Electr 2:1066–1076.
Wang MD, Schnitzer MJ, Yin H, Landick R, Gelles J, Block SM. 1998. Force and velocity measured for single molecule of RNA polymerase. Science 282:902–907.
Weiss S. 1999. Fluorescence spectroscopy of single biomolecules. Science 283:1676–1683.
Weiss S. 2000. Measuring conformational dynamics of biomolecules by single molecule fluorescence spectroscopy. Nature Struct Biol 9:724–729.
Yin H, Landick R, Gelles J. 1994. Tethered particle motion method for studying transcript elongation by a single RNA polymerase molecule. Biophys J 67:2468–2478.
Yin H, Wang MD, Svoboda K, Landick R, Block SM, Gelles J. 1995. Transcription against an applied force. Science 270:1653–1657.
Yin H, Artsimovitch I, Landick R, Gelles J. 1999. Nonequilibrium mechanism of transcription termination from observations of single RNA polymerase molecules. Proc Natl Acad Sci USA 96:13124–13129.